Exploring Lattice Defects in Palladium and Its Alloys Using Dissolved Hydrogen

PART II: HYDROGEN SEGREGATION TO INTERNAL INTERFACES AND TO INHOMOGENEOUS REGIONS

By Ted B. Flanagan

Materials Science Program and Chemistry Department, University of Vermont, Burlington, VT 05405, U.S.A.

R. Balasubramaniam

Department of Materials and Metallurgical Engineering, Indian Institute of Technology, Kanpur, 208 016, India

and R. Kirchheim

Institut für Materialphysik, Hospitalstrasse 3–7, 37073 Göttingen, Germany

The first part of this paper, published in the July issue of this Journal, described the combination of physical metallurgical techniques and hydrogen solubilities used to help in characterising defects in palladium (Pd) and Pd alloys. In this second part, the solubilities of hydrogen (H_2) in internally oxidised Pd alloys are discussed. Internal oxidation, for example of a palladium-aluminium alloy, results in the formation of small alumina precipitates within the Pd matrix. Dissolved H in the alloy is strongly trapped at the metal/oxide interface. This can be detected by deviations in H solubility from that expected for Pd. Hydrogen in Pd and its alloys has been modelled mathematically as the occupation by H atoms of interstitial sites within fixed metal sublattices. However, recently it has been realised that at moderately high temperatures and H_2 pressures some alloy lattices are not fixed, as the dissolved H promotes metal atom diffusion. This results in phase separation in some alloys, for example (Pd + Pt + H), according to a ternary equilibrium. The dissolved H can be removed from such alloys at low temperatures allowing the metastable, phase-separated alloy lattices to be characterised via measurements of H_2 solubilities and suitable physical metallurgical techniques.

Alloys containing solutes that are more readily oxidised than their solvent metal can be internally oxidised in oxygen gas (O_2(g)) at elevated temperatures ≥ 1000 K. The oxidation results in the formation of essentially pure metal matrices containing nanometre-sized internal oxide precipitates. In effect, a metal/oxide composite is formed (39). Binary palladium (Pd) alloys with solute metals, such as aluminium (Al), magnesium (Mg) and zirconium (Zr), have been internally oxidised to form essentially pure Pd matrices containing second phases of nanosized oxide precipitates (40–42).

Internal Oxidation of Pd Alloys such as Palladium-Aluminium

After internal oxidation of, for example, a $Pd_{0.97}Al_{0.03}$ alloy, nanocrystalline alumina precipitates are visible in TEM photomicrographs. The size of the precipitates is greater after internal oxidation of *Pd*-Al alloys (Pd is the majority element in the alloy) at 1273 K than at 1073 K (17, 40, 42, 43). Huang found that the precipitates resulting from oxidation at 983 K were about one tenth as large as those from internal oxidation at 1273 K (17).

Internal oxidation of alloys proceeds by dissociation of O_2(g) at the alloy surface, diffusion of interstitial O atoms into the alloy, oxidisation of the solute atoms and their agglomeration into oxide precipitates. In order to relieve the internal compressive stress resulting from the growth of the oxide precipitates, metal atoms are transported from the metal/oxide interface to the surface and vacancies must therefore be transported in the opposite direction during the process of internal oxidation (44, 45). Palladium nodules have been

observed at the surface and on grain boundary walls resulting from the internal oxidation of *Pd*-Al alloys (46).

It has been shown that the kinetics of H_2 absorption are enhanced after internal oxidation of *Pd*-Al alloys (47). Internal oxidation thus appears to be a convenient method of obtaining enhanced kinetics for Pd and for some Pd alloys, particularly *Pd*-Ag. It may, for instance, provide a means for obtaining improved diffusion membranes. There is also some evidence that the internal oxidation of *Pd*-Al alloys renders them more resistant to CO poisoning than before their internal oxidation (48).

H_2 Solubility in Internally Oxidised Pd Alloys (Pd/MO_x Composites)

The total area of the Pd/oxide interface in internally oxidised alloys can be several m^2 per cm^3 of alloy (49). These internal metal/oxide interfaces are generally free from impurities and so provide a way to investigate the segregation of solutes to impurity-free interfaces. Huang, Kirchheim and coworker were the first to investigate the segregation of hydrogen atoms to Pd/oxide interfaces in internally oxidised alloys of *Pd*-Mg, *Pd*-Al and other Pd-rich alloys (41). Electrochemical methods were employed to measure the relative H chemical potentials

$$\Delta\mu_H = \mu_H - 1/2\mu^\circ_{H_2}$$

as a function of r. $\Delta\mu_H - r$ relationships were obtained for internally oxidised alloys in the very dilute solution region where H trapping at the interface is most important; μ_H is the chemical potential of an isolated dissolved H in the solid phase, $\mu^\circ_{H_2}$ is the chemical potential in the gaseous phase, and r is the H/Pd atom ratio. $\Delta\mu_H$ is very negative for this H trapping and the differences in these relationships for pure Pd and the internally oxidised alloys gives the amounts of trapped H.

More recently, Flanagan, Balasubramaniam and their coworkers (42, 43) introduced H *via* the gas phase to measure $\Delta\mu_H - r$ relationships in the dilute and concentrated H phases of internally oxidised *Pd*-Al. Aside from the very dilute trapping region, the H_2 isotherms for internally oxidised *Pd*-Al alloys corresponded very closely to those for pure Pd. This confirms that all the Al has been oxidised to form alumina precipitates within an essentially pure Pd matrix, that is, a metal/ceramic composite is formed (42).

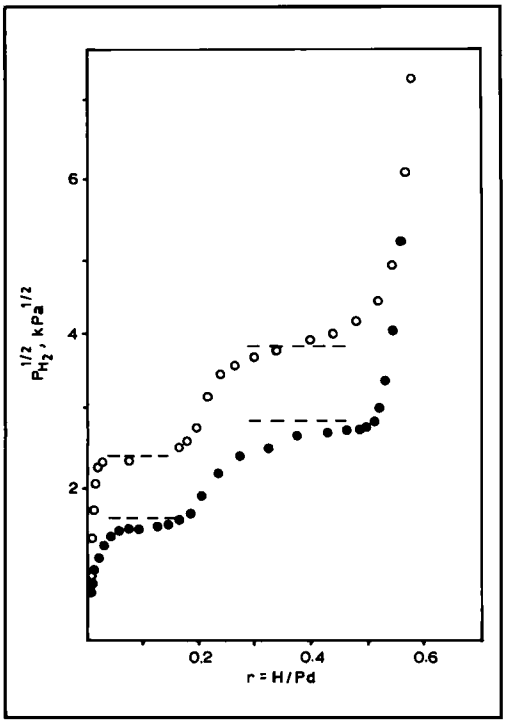

Fig. 6 H_2 isotherm (323 K) for a partially internally oxidised $Pd_{0.97}Al_{0.03}$ alloy.
The lower set of horizontal dashed lines are plateau pressures for the oxidised part of the alloy, Pd-H.
The upper set of horizontal dashes are for the unoxidised $Pd_{0.97}Al_{0.03}$ alloy.
o *absorption of H_2;*
• *desorption of H_2*

A *partially* internally oxidised *Pd*-Al alloy has two plateaux in its isotherm, one for the internally oxidised portion, Pd-H, and the other for the unoxidised portion, as seen in Figure 6 for a $Pd_{0.97}Al_{0.03}$ alloy. The two plateaux demonstrate the interfacial nature of the internal oxidation because if internal oxidation took place homogeneously there would be only one plateau with a hydrogen pressure (p_{H_2}) between the pressures of Pd and the $Pd_{0.97}Al_{0.03}$ alloy. The relative lengths of the plateaux in Figure 6 can be used to obtain the fraction of internal oxidation, while the transition region between the two plateaux provides

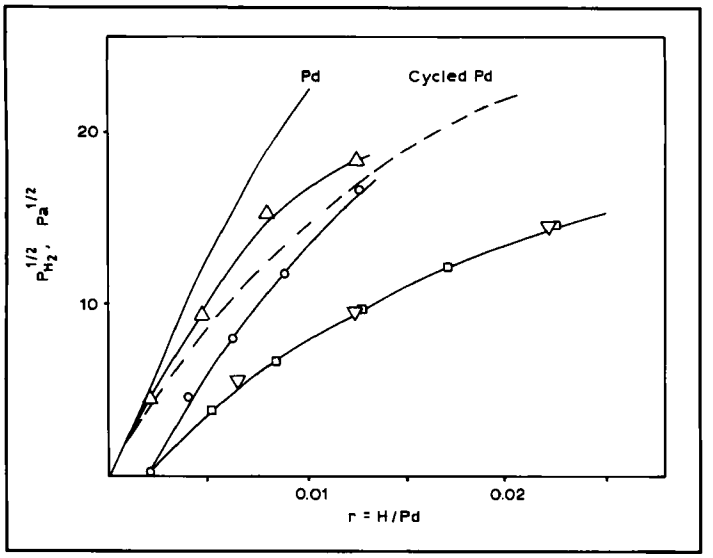

Fig. 7 Dilute phase H_2 isotherms (taken at 273 K) for an internally oxidised (1073 K, 72 h) $Pd_{0.97}Al_{0.03}$ alloy.
o after internal oxidation;
Δ repeat measurement of the dilute solubility after evacuation at 323 K;
□ solubility after cycling and evacuation at 323 K;
∇ repeat measurement after evacuation at 323 K of the cycled alloy (50)

information about the diffuseness of the interface and the metal atom diffusion constants.

Dilute phase H_2 solubilities (at 273 K), which indicate that H has been strongly trapped at the Pd/Al_2O_3 interface, are shown in Figure 7 for an internally oxidised (at 1073 K) $Pd_{0.97}Al_{0.03}$ alloy (50). The initial solubility has an intercept along the *r* axis at 0.002 which corresponds to the interfacially trapped H, in agreement with the electrochemical results of Huang *et al.* (41). While still in the dilute phase, the alloy was evacuated (at 323 K); the remeasured solubility data pass through the origin showing that only the strongly trapped H cannot be removed by evacuation at 323 K.

In addition to the strong H trapping at the interface where essentially $p_{H_2} = 0$, there is a solubility enhancement in the dilute region, which is attributed to H segregation in the stress field about the precipitates. The stress field results from cooling the two-phase material (Pd/Al_2O_3 which has two different coefficients of thermal expansion) from its high oxidation temperature. Calculations

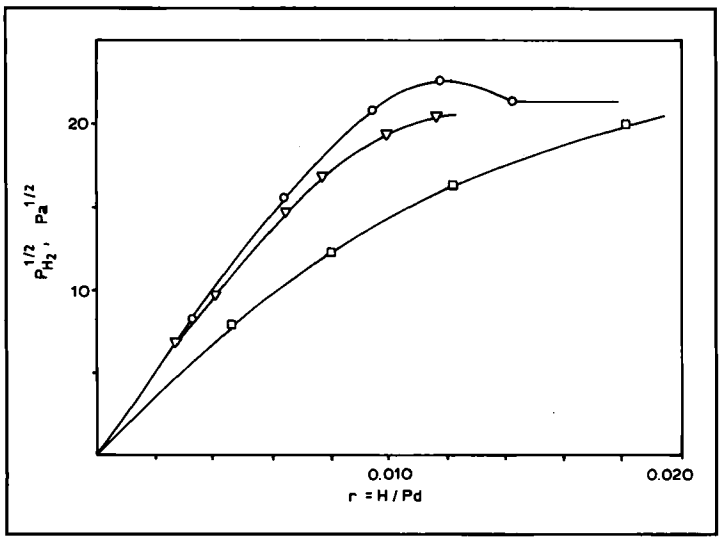

Fig. 8 Dilute phase H_2 isotherms for Pd.
o initial solubility in well-annealed Pd;
□ solubility after cycling;
∇ solubility after annealing the cycled Pd for 24 h at 723 K

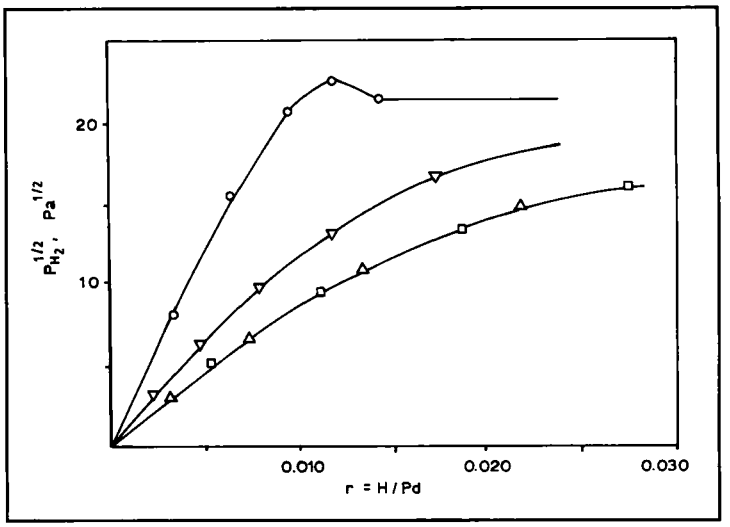

Fig. 9 Dilute phase H_2 isotherms (273 K) for an internally oxidised (1073 K, 72 h) $Pd_{0.97}Al_{0.03}$ alloy and annealed Pd.
o initial solubility of annealed Pd;
∇ after internal oxidation of the $Pd_{0.97}Al_{0.03}$ alloy;
Δ after cycling the internally oxidised $Pd_{0.97}Al_{0.03}$ alloy;
□ after annealing the cycled internally oxidised $Pd_{0.97}Al_{0.03}$ alloy at 823 K for 48 h.
Where necessary data have been translated along the r axis by −0.002 for the alloy in order to intersect the origin and to focus attention on the H-dislocation segregation

made on the basis of this thermal residual stress give reasonable agreement with experiment (43).

The internally oxidised $Pd_{0.97}Al_{0.03}$ alloy was cycled through the hydride phase and evacuated (at 323 K). In contrast to the solubility remeasured after evacuation at 323 K, there is again a positive intercept on the *r* axis, indicating that the strongly trapped H can be removed by cycling and evacuation (323 K), but not by just evacuation (Figure 7). The H, which initially was strongly trapped, was shown not to be present after cycling – none was evolved when the cycled, internally oxidised alloy was heated to 573 K. However, trapped H *is* evolved by such heating of an uncycled internally oxidised alloy (50). Dislocations in the vicinity of the interfaces, resulting from cycling, may decrease the depth of the potential wells and allow the initially strongly trapped H to be removed.

Annealing of Dislocations in Pd and in Cycled, Internally Oxidised *Pd*-Al

Annealing at 623 K (24 h) causes a decrease in the hydrogen solubility enhancement of Pd which has been cycled and a decrease in the dislocation density – judging from TEM photomicrographs. After annealing cycled Pd at 723 K (24 h), its H_2 solubility returns almost to that of well-annealed Pd (Figure 8). These results show that dislocations become mobile in pure Pd at ≥ 623 K allowing them to rearrange and to annihilate sufficiently to reduce the dislocation density and solubility enhancement.

TEM photomicrographs show only small dislocation densities in internally oxidised *Pd*-Al alloys (17, 40, 42). However, after hydriding/dehydriding (cycling), large dislocation densities and extensive intergranular cracking appear (51). Dilute phase solubilities (273 K) for an internally oxidised (1073 K, 72 h) $Pd_{0.97}Al_{0.03}$ alloy (a Pd/Al_2O_3 composite) were measured before and after cycling (Figure 9). Cycling the internally oxidised alloy leads to a greater solubility enhancement than cycling Pd does; this is consistent with reports of increased dislocation densities from cold working metals which contain small internal precipitates (52, 53).

Internal oxidation is of practical value because it is used for dispersion hardening of alloys (39). In contrast to Pd (Figure 8), when the cycled internally oxidised $Pd_{0.97}Al_{0.03}$ alloy was annealed for 48 h *in vacuo* at 823 K, there was no change in its solubility enhancement (Figure 9). The dislocations in this internally oxidised alloy are therefore immobile even though the annealing temperature is higher and the time taken was longer than that used for cycled Pd (24 h) where the solubility enhancement nearly vanished (Figure 8).

A $Pd_{0.97}Al_{0.03}$ alloy, internally oxidised at 1273 K and cycled, was annealed at 823 K for 48 h. After this its solubility enhancement almost completely disappeared in contrast to the alloy internally oxidised at 1073 K. This is in keeping with the

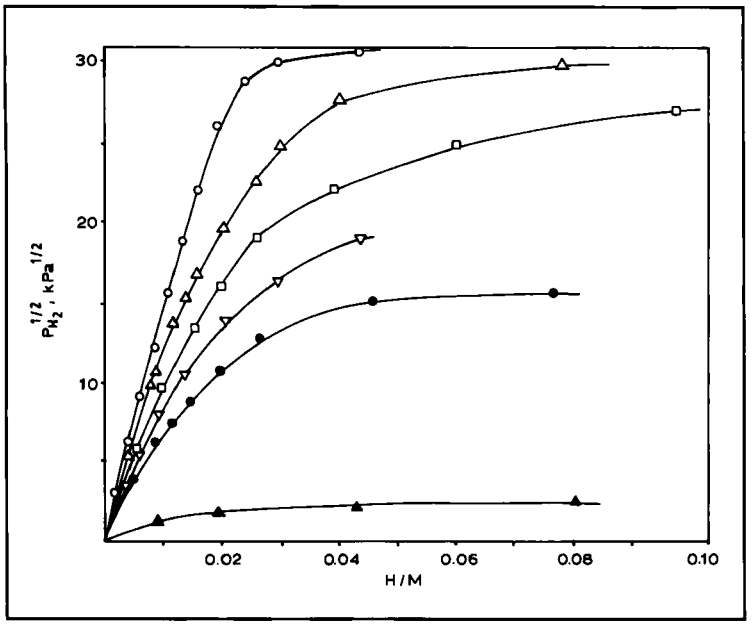

Fig. 10 Dilute phase H_2 solubilities (303 K) for a $Pd_{0.80}Rh_{0.20}$ alloy cooled from ≈ 1100 K at different rates or heat treated in vacuo at 873 K or in H_2 (100 MPa).
○ quenched;
△ rapid cooling in air;
□ slowly cooled in furnace;
▽ heated in vacuo for 12 days at 873K;
● treated in H_2 (12 days, 5.5 MPa, 873 K);
▲ treated in H_2 (5 h, 100 MPa, 673 K) (redrawn after (56))

expectation that the small, closely spaced precipitates resulting from internal oxidation at 1073 K interact strongly with dislocations, while the more widely spaced and larger precipitates from internal oxidation at 1273 K do not (45).

H-Induced Phase Separation of Palladium-Rhodium Alloys

Unlike most other binary f.c.c. Pd alloys whose H_2 solubilities have been studied, the Pd/Rh alloy system has a miscibility gap with a critical temperature of ~ 1120 K. At 873 K, for example, the coexisting phases have Rh atom fractions of about 0.12 and 0.87 (54, 55). Using X-ray diffraction (XRD), Raub *et al.* (54) showed that at 873 K the phase separation is extremely slow: 63 days of annealing were required for a $Pd_{0.49}Rh_{0.51}$ alloy, while a $Pd_{0.74}Rh_{0.26}$ alloy had not phase-separated after 1 year. However, H_2 solubilities are more sensitive than XRD for detecting a phase separation.

In Figure 10, H_2 solubilities (303 K) following the cooling of a $Pd_{0.80}Rh_{0.20}$ alloy at different rates from elevated temperatures are shown. Significant solubility differences can be seen between alloys prepared:

- by quenching
- by relatively rapid cooling from ≈ 1000 K and
- by slower cooling from 873 K.

A greater solubility at a given p_{H_2} indicates that there is a greater degree of phase separation. Noh *et al.* (56) showed that metal atom diffusion, and consequently phase separation, is greatly accelerated by dissolved H_2. This is the reason why there is a greater dilute-phase H_2 solubility after the alloy is heated at 673 K in the presence of 100 MPa H_2 (Figure 10), than after treatments under H-free conditions.

Fukai and coworkers (57) have shown that at ultra high p_{H_2} (5 GPa) a $Pd_{0.80}Rh_{0.20}$ alloy separates into two phases in 120 seconds at 873 K, according to the phase diagram. It is clear that dissolved H at ≥ 673 K greatly accelerates the phase separation of metastable, homogeneous *Pd*-Rh alloys (56–58).

Other Palladium Alloys

Palladium-metal (M) alloys, which are not metastable, have been found to phase-separate in the presence of H_2 at relatively moderate temperatures. For these alloys phase separation can occur *via* a ternary (Pd + M + H) equilibrium which can be established at a sufficiently high p_{H_2} for appreciable H to dissolve. M is a solute such as platinum (Pt), nickel (Ni), or cobalt (Co) where the plateau pressures p_{H_2} of the alloy are greater than for Pd-H

and thus phase separation leads to a lower free energy. By contrast, for Pd alloys where the plateau pressures p_{H_2} are lower than for Pd-H, phase separation *via* a ternary equilibrium has not been observed (59, 60). For alloys such as *Pd*-Pt, H has both an equilibrium and a kinetic role, however, for the metastable *Pd*-Rh alloys, the kinetic role appears to be dominant.

$Pd_{0.80}Pt_{0.20}$ is an example of an alloy where phase separation occurs *via* a (Pd + M + H) ternary equilibrium. After phase separation by H_2 treatment at 100 MPa (673 K) and subsequent low temperature removal of H, H_2 isotherms (273 K) were measured on the metastable, phase-separated alloy and compared to isotherms for the homogeneous alloy before the H_2 treatment (Figure 11). Before the H_2 treatment there is no plateau region because of the relatively large fraction of Pt. After the H_2 treatment there is a well-defined plateau reflecting the separated Pd-rich phase.

It should be emphasised that the dissolved H must also have a kinetic role because usually metal atom equilibrium would not be expected to be readily established at 673 K.

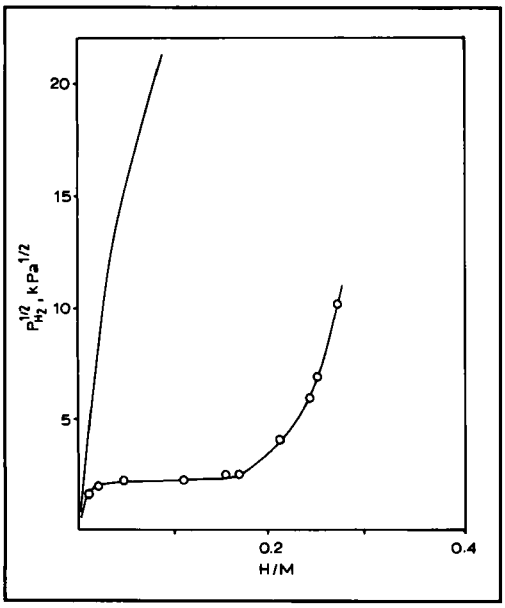

Fig. 11 H_2 isotherms (273 K) for a $Pd_{0.80}Pt_{0.20}$ alloy. Continuous line is for the homogeneous alloy; o after treatment in 100 MPa H_2 for 3 h at 673 K (redrawn from (59))

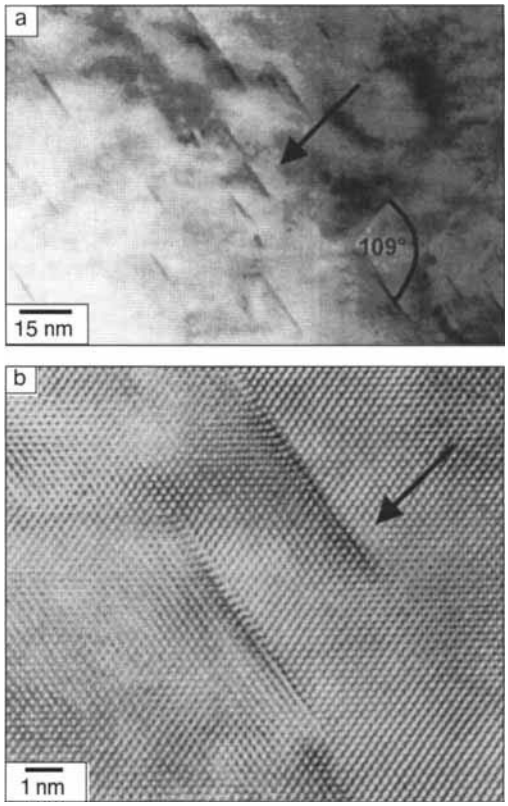

Fig. 12 HREM images for a $Pd_{0.80}Pt_{0.20}$ alloy after treatment with H_2 at 100 MPa for 3 h at 673 K. Two different magnifications are shown in (a) and (b). The illumination is parallel to the [011] zone axis. Before the H_2 treatment, the lattice appears to be perfect (61)

This phase separation is on a fine scale not detectable by XRD, however, it has been detected by small angle neutron scattering (SANS) (59) and, very recently, by high resolution electron microscopy (HREM) (61). Using the latter method, small Pt-rich precipitates were observed within a Pd-rich matrix after a H_2 treatment (673 K) (Figure 12). These HREM results directly confirm the indirect evidence from the H_2 isotherm measurements (Figure 11).

Values for the H diffusion constants, measured before and after H_2-treatment of the $Pd_{0.80}Pt_{0.20}$ alloys, also support the occurrence of phase separation. It is known that the diffusion constants of H in f.c.c. Pd-rich alloys decrease with increase of solute concentration (62) and, since diffusion is found to be faster after the H_2-treatment, it

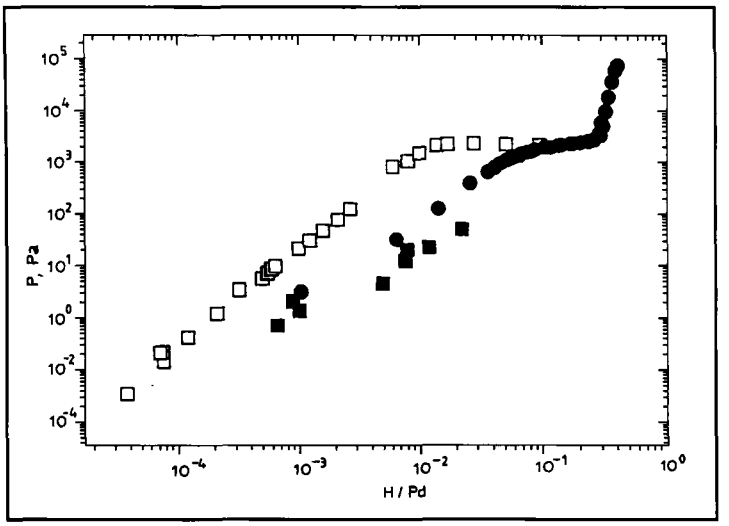

Fig. 13 Experimental solubility data at 310 K for H_2 solubility in a 3.1 nm Pd cluster. Open symbols indicate absorption; filled symbols indicate desorption (68)

follows that the majority of the diffusion occurs within a principal phase which must have a lower Pt content than the original alloy.

Effect of Crystallite Size on Hydrogen Solubility in Pd

On decreasing the crystallite size of materials the realm of nanostructured and cluster materials is reached. Nanostructured materials consist of small crystallites (typically of sizes 30 nm or less) joined together by grain boundaries. Their properties are quite different from those of bulk material due to the large fraction of interfaces present. Clusters are agglomerates of a few hundred to a few thousand atoms whereas nanocrystallites consist of many times that number.

Frieske and Wicke (63) reported that H_2 isotherms for Pd black shift from the origin to start the normal dilute phase solubility at a higher r value due to chemisorption. Hysteresis was reduced for Pd black although the average plateau p_{H_2} was unchanged. Using Pd blacks of various sizes (determined by electron microscopy to be in the range from 113 to 7 nm), Everett and Sermon (64) found a decrease in hysteresis with decrease of crystallite size.

Experimental studies of H_2 absorption by nanocrystalline Pd (n-Pd) have been reported (65–67). When compared to bulk Pd, the notable features of H_2 solubility in nanocrystalline Pd are the enhanced solubilities in the α-phase (65–68) and a narrowing of the two-phase field (66) while the average plateau p_{H_2} appears largely unchanged from that of bulk Pd. It was suggested that the enhanced H_2 solubility in the dilute phase of n-Pd results from H solution in the grain boundaries, which have a spectrum of interstitial site energies and therefore, like amorphous alloys, cannot form a hydride phase (65, 66).

However, using high-resolution X-ray powder diffraction with synchrotron radiation, Eastman *et al.* (69) concluded that both the bulk and the grain boundary material in n-Pd converted to the hydride phase. They attributed the narrowing of the two-phase field to a decrease in the ratio of the entropy-of-mixing to the enthalpy-of-mixing of H in n-Pd, thereby shifting the Pd-H critical temperature to a lower value (69). Since suitable values chosen for the thermodynamics of mixing can generate any desired simple miscibility gap phase diagram, agreement with experiment is not meaningful. Further work must be done to resolve this controversy regarding the narrowing of the phase diagram.

A H_2 isotherm was measured volumetrically for the first time by Pundt *et al.* (68) for Pd clusters (3.1 nm-size embedded in two different types of elastically soft matrices – a soft polymer matrix and a surfactant shell) (Figure 13). The dilute phase solubility of H_2 in the Pd clusters was greater than in

bulk Pd (Figure 13). This was explained based on the available subsurface sites in the clusters having a different energy with respect to interstitial H than bulk Pd sites (68). Zütel *et al.* (70) utilised ligand-stabilised Pd clusters (produced by a reduction method) mixed with Cu powders as electrodes for the determination of the H capacities; the solubilities were found to decrease with cluster size as expected from the n-Pd behaviour.

Conclusions

The usefulness and convenience of H_2 solubilities for investigating lattice defects, including inhomogeneities, in Pd and its alloys has been described. H_2 solubilities can show that large dislocation densities form by cycling Pd and Pd/Al_2O_3 composites (prepared by internal oxidation at 1073 K) through the hydride phase changes. H_2 solubilities also show that the dislocation density of Pd is significantly reduced by annealing at 723 K whereas the dislocation density of the Pd/Al_2O_3 composite is not. Thus H_2 solubilities can readily monitor metallurgical phenomena such as dislocation annihilation.

Studying the segregation of solutes to internal interfaces is important because of the wide occurrence of metal/oxide interfaces in technology. Hydrogen could therefore become a facet helping in the characterisation of industrial small-scale materials.

In addition to simply dissolving in metals and alloys, H can have the role of enhancing metal atom diffusion leading to phase separation, according to a ternary equilibrium, in some Pd-alloys. Upon cooling and removal of the H, the metal atoms remain 'frozen' and have been shown to be phase separated by hydrogen isotherms, SANS and HREM methods.

Nanoscience is a rapidly developing field, believed to have some important industrial applications. The study of H_2 solubilities in nanocrystalline Pd and its alloys may well be a useful tool for their characterisation. For example, the question of whether or not the smaller plateau in n-Pd indicates that the grain boundary Pd is disordered and cannot form the hydride phase is important for understanding nanometals. Hydrogen absorption by Pd will be better and more fully understood if its study is extended to as many different forms of Pd as possible.

Acknowledgements

The authors wish to acknowledge the invaluable help from many of their students and coworkers.

References

39 J. Meijering, "Advances in Materials Research", ed. H. Herman, Vol. 5, Wiley, New York, 1971, p. 1

40 J. Eastman and M. Ruhle, *Ceram. Eng. Sci. Proc.*, 1989, **10**, 1515

41 X. Y. Huang, W. Mader and R. Kirchheim, *Acta Metall. Mater.*, 1991, **39**, 893

42 H. Noh, T. Flanagan, R. Balasubramaniam and J. Eastman, *Scr. Mater.*, 1996, **34**, 665

43 R. Balasubramaniam, H. Noh, T. Flanagan and Y. Sakamoto, *Acta Metall. Mater.*, 1997, **39**, 893

44 J. Mackert, R. Ringle and C. Fairhurst, *J. Dent. Res.*, 1983, **62**, 1229

45 S. Guruswamy, S. Park, J. Hirth and R. Rapp, *Oxid. Met.*, 1986, **26**, 77

46 R. Balasubramaniam, R. Kirchheim, D. Wang and T. Flanagan, *J. Alloys Compd.*, 1999, **293–295**, 306

47 D. Wang, J. Clewley, T. Flanagan, Y. Sakamoto and K. Shanahan, *J. Alloys Compd.*, 2000, **298**, 261

48 T. Flanagan, D. Wang and K. Shanahan, *Phys. Chem. Chem. Phys.*, 2000, **2**, 4976

49 J. Gegner, G. Horz and R. Kirchheim, *Interface Sci.*, 1997, **5**, 231

50 D. Wang, T. Flanagan and R. Balasubramaniam, to be published

51 T. Flanagan, R. Balasubramaniam and Y. Sakamoto, to be published

52 M. Klein and R. Huggins, *Acta Metall.*, 1962, **10**, 55

53 M. Lewis and J. Martin, *Acta Metall.*, 1963, **11**, 1207

54 E. Raub, H. Beeskow and D. Menzel, *Z. Metallkd.*, 1959, **50**, 426

55 J. Shield and R. Williams, *Scr. Met.*, 1987, **21**, 1475

56 H. Noh, J. Clewley, T. Flanagan and A. Craft, *J. Alloys Compd.*, 1996, **240**, 235

57 K. Watanabe, N. Okuma, Y. Fukai, Y. Sakamoto and Y. Hayashi, *Scr. Mater.*, 1996, **34**, 551

58 T. Flanagan and C.-N. Park, *J. Alloys Compd.*, 1999, **293–295**, 161

59 T. Flanagan, J. Clewley, H. Noh, J. Barker and Y. Sakamoto, *Acta Metall.*, 1998, **46**, 2173

60 T. Flanagan, H. Noh, J. Clewley and J. Barker, *Scr. Met.*, 1998, **39**, 1607

61 R. Lüke, G. Schmitz, T. Flanagan and R. Kirchheim, *J. Alloys Compd.*, in press

62 E. Wicke and H. Brodowsky, "Hydrogen in Metals", eds. G. Alefeld and J. Völkl, Vol. 2, Springer-Verlag, Heidelberg, 1978

63 H. Frieske and E. Wicke, *Ber. Bunsenges Phys. Chem.*, 1973, **77**, 48

64 D. Everett and P. Sermon, *Z. Phys. Chem. NF*, 1979, **114**, 101

65 T. Mütschele and R. Kirchheim, *Scr. Metall.*, 1987, **21**, 135

66 T. Mütschele and R. Kirchheim, *op. cit.* (Ref. 65), p. 101

67 H. Natter, B. Wettmann, B. Heisel and R. Hempelmann, *J. Alloys Compd.*, 1997, **253–254**, 84

68 A. Pundt, C. Sachs, M. Winter, M. Reetz, D. Fritsch and R. Kirchheim, *J. Alloys Compd.*, 1999, **293–295**, 480

69 J. Eastman, L. Thompson and B. Kestel, *Phys. Rev. B*, 1993, **48**, 84

70 A. Züttel, Ch. Nützenadel, G. Schmid, D. Chartouni and L. Schlapbach, *J. Alloys Compd.*, 1999, **293–295**, 472

The Authors

Ted B. Flanagan is Professor of Chemistry at the University of Vermont, U.S.A. His main interests are the thermodynamics of metal hydrogen systems and H-induced lattices changes.

R. Balasubramaniam is Associate Professor of Materials and Metallurgical Engineering at the Indian Institute of Technology, Kanpur, India. His interests include the effect of H on materials and archeological metallurgy.

R. Kirchheim is Director of the Institut für Materialphysik, Göttingen, Germany. His main interests encompass the physics of materials in particular the role of H in characterising defective and nanosized metals and alloys.

Hydrogen Detection with a Palladium-Nickel HSGFET

There are now vehicles on our roads run by hydrogen (H)-powered fuel cells, and H_2 is predicted to have a far more important role as an energy source in the future. Hydrogen is a highly flammable gas, and being odourless and colourless is not detectable by human olfactory and other senses. Therefore to have sensors able to detect it rapidly and accurately in the atmosphere is very important. This is particularly critical at high H_2 concentrations before ignition concentrations are reached.

One method of sensing could be to measure the work function change due to H physisorption or chemisorption on a gas sensitive layer. As the response to bulk effects is almost negligible, the measurements could be carried out at low temperatures, in contrast to the usual conductance sensors which work at very high temperatures. A new type of gas sensor may then be constructed, utilising a hybrid suspended gate field effect transistor (HSGFET), of low power demand (< 10 mW). Pd-MOS based H sensors are already known, but when operated at high H_2 concentrations the Pd film blisters. If Pd alloys are used instead of Pd there is a possibility that blistering could be eliminated.

A team of researchers from Germany, Sweden and India have now attempted to improve the stability of HSGFETs up to high H_2 concentrations, by replacing Pd by a thin layer of Pd-Ni or Pd-Ag alloy (K. Scharnagl, M. Eriksson, A. Karthigeyan, M. Burgmair, M. Zimmer and I. Eisele, *Sens. Actuators B, Chem.*, 2001, **78**, (1–3), 138–143).

Pd-Ni and Pd-Ag films were grown onto titanium-coated silicon wafers in UHV chambers at a base pressure of 1×10^{-10} Torr by co-evaporation techniques. Work function measurements and time responses on exposure to H_2 and other commonly found environmental gases were then carried out.

It was found possible to detect H_2 concentrations of up to 2% at room temperature without blister formation, when Pd-Ni alloy was used as the gas sensitive material. The response to 2% H_2 was ~ 500 mV in dry conditions, but less than half this value with moistened carrier gas, however then the desorption time was lowered. The Pd-Ag alloy was not stable and is not suitable as a sensor material. The Pd-Ni alloy, in addition to having a low cross-sensitivity to other gases, seems to be a promising material for room temperature H monitoring.

Tailored Palladium/Silica Spheres

The ability to control the preparation of porous materials used as supports is important in the fields of heterogeneous catalysis and molecular sieving. Templates of colloidal silica crystals and anion exchange resins have resulted in controlled pore sizes and macrostructures.

Now, researchers from Sweden report the synthesis of Pd-containing silica spheres prepared by using anion exchange resins as templates (L. Tosheva and J. Sterte, *Chem. Commun.*, 2001, (12), 1112–1113).

Their method is based on the fact that the resin-silica composite, obtained after the ion exchange of silica species, retains a high anion exchange capacity. This allows the introduction of negatively charged ions, such as $PdCl_4^{2-}$. Calcination removes the resin bead template and the Pd is converted to an oxide form. Hard, solid silica spheres with a controllable amount of Pd can be prepared by this technique. With their high surface areas and large pore volumes, these materials may be useful for catalytic applications.